



Hybrid Simulation of Thermomechanical Structural Response

Catherine A. Whyte¹; Kevin R. Mackie, M.ASCE²; and Bozidar Stojadinovic³

Abstract: A new thermomechanical hybrid simulation method is proposed that extends the mechanical hybrid simulation method by including thermal degrees of freedom and temperature loads. The thermomechanical hybrid simulation method was implemented in the OpenSees and OpenFresco frameworks. Modifications to enable this new capability centered on incorporating the temperature degrees of freedom in the hybrid model domain, and on developing new OpenFresco objects and a test execution strategy to simultaneously control the structural elements of the experimental setup, the thermal loads, and the mechanical loads. The implementation of the thermomechanical method at the ETH Zürich IBK Structural Testing Laboratory was verified and validated using a simple two-element hybrid model. The responses of the model to a force ramp, applied to the full structure, and a scaled version of the ISO 834 standard fire curve, applied to the experimental element, were obtained in two simulations—one conducted using an explicit and the other using an implicit integration scheme. The tests yield very similar results, and both simulations closely match the theoretical solution. DOI: [10.1061/\(ASCE\)ST.1943-541X.0001346](https://doi.org/10.1061/(ASCE)ST.1943-541X.0001346). © 2015 American Society of Civil Engineers.

Author keywords: Metal and composite structures.

Introduction

Hybrid Simulation of Response to Mechanical Loads

Hybrid simulation is a method to investigate the structural response to mechanical loads imposed on a hybrid model of a prototype structure. The portions of the prototype structure whose behavior is understood well are generally modeled using standard finite elements, while the portions of the structure whose behavior is highly nonlinear or not well understood are modeled using experimental elements. These experimental elements interface with physical specimens through laboratory test setups. The response of the hybrid model to load over the time domain of interest is computed by solving the equations of motion of the entire hybrid model using a time-stepping integration process. Computer control software and the specimen actuation system maintain the deformation compatibility and force equilibrium conditions at the interfaces between the numerical and physical portions of the hybrid model. The method originated as the computer-actuator online system (Takanashi et al. 1975) or the pseudodynamic testing method

(Mahin and Williams 1981; McClamroch et al. 1981). A comprehensive review of the hybrid response simulation method is presented by Saouma and Sivaselvan (2008).

When a displacement control approach is used in hybrid simulation, the computed displacements of the experimental elements in the hybrid model are applied to the physical specimens at each time step. The restoring forces are measured using load cells and sent back to the hybrid model. This feedback data is used to compute the displacements in the next time step, so the displacement sequences applied to the physical substructures are not known a priori. Thus, hybrid simulation is more realistic than a quasi-static cyclic test, where a predetermined load sequence is defined to match the numbers and amplitudes of deformation cycles that the specimen is expected to experience during a typical earthquake. To date, hybrid simulation has been used to investigate the dynamic response of structures to earthquake ground motion excitation, including the response to multiple earthquake sequences (Whyte and Stojadinovic 2014) and to postearthquake traffic loads (Terzic and Stojadinovic 2014). While the hybrid simulation method has been assumed to be applicable to other dynamic mechanical loads, such as wind, blast, impact, waves, and traffic, few theoretical investigations or experimental implementations have been carried out to expand the method beyond seismic loading.

Standard Fire Testing

Large-scale structural fire tests (Chen et al. 2012; Kirby 1997; Kitano et al. 2000) are rare because they require specialized facilities. High costs are associated with use of those facilities, construction of large-scale specimens, and accurately measuring structural response at high temperatures. Most experiments that investigate structural performance in fire have been performed on individual components (e.g., Dwaikat et al. 2011; Franssen et al. 1995; Garner and Baddoo 2006; Lie 1989; Martins and Rodrigues 2010; Tondini et al. 2013). A standard fire resistance test (Lawson 2009) is performed on a single, simply supported structural element in a furnace, usually for the purpose of determining a fire rating for that element. This specimen is held under a constant, usually gravity,

¹Postdoctoral Researcher, Institute of Structural Engineering, Dept. of Civil, Environmental and Geomatic Engineering, Swiss Federal Institute of Technology (ETH) Zürich, HIL E13.1, Stefano-Francini-Platz 5, CH-8093 Zürich, Switzerland (corresponding author). E-mail: whyte@ibk.baug.ethz.ch

²Associate Professor and Associate Chair, Dept. of Civil, Environmental, and Construction Engineering, Univ. of Central Florida, Engr II 402, 4000 Central Florida Blvd., Orlando, FL 32816-2450. E-mail: kmackie@mail.ucf.edu

³Professor and Chair of Structural Dynamics and Earthquake Engineering, Dept. of Civil, Environmental and Geomatic Engineering, Swiss Federal Institute of Technology (ETH) Zürich, HIL E14.1, Stefano-Francini-Platz 5, CH-8093 Zürich, Switzerland. E-mail: stojadinovic@ibk.baug.ethz.ch

Note. This manuscript was submitted on September 24, 2014; approved on April 28, 2015; published online on July 22, 2015. Discussion period open until December 22, 2015; separate discussions must be submitted for individual papers. This paper is part of the *Journal of Structural Engineering*, © ASCE, ISSN 0733-9445/04015107(11)/\$25.00.

load while the furnace is heated following an increasing temperature-time curve. The international standard ISO 834 temperature-time fire curve is defined in the Eurocode 1 Part 1-2 (CEN 2002) as

$$\Theta_g = 20 + 345 \log 10(8t + 1) \quad (1)$$

where Θ_g = temperature ($^{\circ}\text{C}$) in the fire compartment; and t = time (min). Though such component tests provide important information for understanding fire performance of specific structural elements, they do not give information about how complete structures perform in actual fire scenarios (Wang 2002).

Hybrid Fire Testing

A hybrid fire test (HFT) can provide meaningful information about the behavior of a complete structure. Here, a standard fire test of a specific component or components is combined with a numerical model of the remainder of the structure. The boundary conditions of the physically tested substructure are adjusted to match the behavior of the numerical model in a feedback loop. The process of substructuring enables examination of the behavior of a whole structure exposed to fire and mechanical loads. It also enables parametric tests of different structural configurations.

A HFT of this nature was proposed and performed by Mostafaei (2013a, b), where the implementation involved human interaction between the numerical and the physical portions of the model. The physical substructure was a first story column, and the numerical substructure was the remaining portion of a 6-story reinforced-concrete building hybrid model. The physical substructure was exposed to both axial loads and elevated temperatures in a furnace chamber. At each 5-min time increment throughout the duration of the test, the axial deformation of the physical column was recorded and manually inserted as the input to the numerical portion of the model. Then the resulting load obtained from the numerical model analysis was recorded and manually commanded to the compression-tension machine to load the column specimen in the furnace.

Hybrid Simulation of Response to Thermal and Mechanical Loads

A new thermomechanical hybrid simulation (TMHS) method is proposed herein. The TMHS method extends the hybrid simulation method to include temperature loads in general, and fire loads in particular. The application of the mechanical and thermal loads is fully computer controlled, thus taking the human out of the simulation. Advantages of the TMHS method include: (1) ability to control many degrees of freedom (DOFs) and work with complex dynamic hybrid models, load combinations, and load sequences; (2) removal of the human from the simulation loop, thus eliminating the possibility of human error; and (3) capability for real-time testing, i.e., conducting a hybrid simulation that accounts for both the rate that captures the development of a fire in a structure (in terms of minutes) as well as the rate that captures the structure's dynamic response (in terms of fractions of a second) to the changes in boundary conditions and load paths as the fire progresses in the prototype structure.

Proof-of-concept TMHS tests were conducted at the Structural Testing Laboratory of the Institute of Structural Engineering (IBK) at the Swiss Federal Institute of Technology (ETH) Zürich, using a simple hybrid model. A single finite-element substructure was implemented in the Open System for Earthquake Engineering Simulation (OpenSees 2015) software framework. The physical substructure was tested in the laboratory in a combined universal

testing machine (UTM), which applied the mechanical loads, and a furnace, which applied the temperature loads. The Open-Source Framework for Experimental Setup and Control (OpenFresco 2015) middleware was extended to link the OpenSees finite-element substructure with the physically tested substructure by transferring both the mechanical and the thermal information at the interface between the substructures. The TMHS method was verified and the TMHS proof-test results validated through a comparison to the theoretical solution for the response of the prototype structure to the applied mechanical and thermal loads.

TMHS Implementation

General Simulation Considerations and Coupling

For assessment of structural response in a compartment fire, first a fire development analysis (FDA), using a zone model or computational fluid dynamics model, propagates the fire and the associated thermal field from the source to the boundaries of structural elements, which are typically modeled only approximately. Analysis of heat and mass transfer in fluid (air) determines the evolution of the fire gas temperatures and the associated radiation field in the building compartment and at the structural element boundaries. This information is transferred to the thermomechanical response analysis (TMRA), which comprises both a heat transfer and a mechanical response analysis. Here, fluid-structure interaction is typically considered in the forms of convection, radiation, and friction at the specimen surfaces to calculate thermal boundary conditions (surface temperatures and thermal fluxes). Then heat transfer by conduction is considered within the structural elements, resulting in the internal temperature fields of individual structural elements. The solution of the mechanical analysis is the strain or displacement fields of the same elements.

There are two different coupling possibilities, both at the macroscopic and microscopic levels. Coupling at the macroscopic scale takes place between the FDA and the TMRA. Either the FDA is performed in its entirety first and passes information to the TMRA (one-way coupling) or the FDA and TMRA exchange information in both directions (two-way coupling). Two-way coupling implies that the TMRA temperature and displacement fields modify the boundaries/input and solution of a subsequent analysis step in the FDA (e.g., damage to partition walls changes the building envelope in FDA), and is not commonly implemented. The FDA generally uses a much higher spatial resolution and a different time scale than the TMRA, which complicates the potential for two-way coupling.

Coupling at the microscopic scale occurs between the thermal and mechanical physics within the TMRA. Typically the heat transfer analysis is performed first (one-way coupling), resulting in a time-dependent internal temperature field. The temperatures induce nonmechanical strains and resisting forces due to temperature-dependent mechanical properties of the materials. However, the mechanical properties of the structure and its deformation and damage states do not influence the temperature, flux, or radiation at the element boundaries and are not returned back to the TMRA heat transfer analysis nor to the FDA. The thermal flux and conduction of heat elsewhere within the element/structure are similarly not returned. Two-way coupling, which is not usually implemented, implies the change in mechanical strains, constitution, damage, or displacement boundaries affect the radiation and conduction. A comprehensive review of these coupling strategies is provided in Tondini and Franssen (2013).

An alternative for structural response analysis is no coupling at either the macroscopic or microscopic scale. A FDA is not performed, but instead, structural element-level thermal strains (or curvatures) are computed for each element in the structure using a predetermined temperature history loading, $T(t)$, and thermal expansion coefficients. The effects of these temperatures on the analytical substructures are typically modeled through fixed-end or element forces. For the experimental substructures, the equivalent structural element deformations are computed numerically and then imposed on the physical specimens using actuators. This simple approach can be implemented without the need for heating the physical specimens, but it does not accurately represent the change in material properties with temperature, nor does it allow the experimental substructures to accurately capture structural behavior under fire loads.

TMHS Approach

To facilitate development and demonstration of TMHS, a proof-of-concept hybrid model was implemented that contains no coupling at the macroscopic scale and one-way coupling at the microscopic scale. However, the proposed TMHS remains general enough to enable one-way and two-way coupling at both the micro and macro scale. A simple two-element hybrid model contains a numerical element, which is unheated (assumed to be insulated from the experimental element and the fire), and an experimental element, which interfaces with a physical specimen, heated in a furnace. The FDA and the thermal analysis are assumed to be completed, resulting in a known temperature history in the physical specimen. The physical specimen is a thin steel specimen with only minor differential between the surface and internal temperature fields, so these are assumed to be the same. Though the standard ISO 834 fire load curve [Eq. (1)] is traditionally used to represent gas temperatures in a furnace, here it is the assumed temperature history at the surface of the physical specimen. Thermocouples on the surface of the physical specimen are used to measure and feedback temperatures, and the temperature control point is located at the mid-height of the specimen. Because the FDA is assumed to be completed, the furnace air temperature does not need to be controlled.

The interactions between the hybrid simulation numerical and experimental substructures are also defined. Mechanically, the numerical and the experimental substructures interact in both directions: displacements are sent to the physical specimen (displacement control), and measured restoring forces are returned to the hybrid model. Thermally, there is a one-way interaction: temperatures are sent to the physical specimen, but thermal fluxes are

not returned to the hybrid model to update its state. Because the numerical element is unheated, it is not necessary to enforce thermal flux equilibrium at the numerical/experimental substructure interface.

Because the hybrid simulation is performed in displacement control, increasing the temperature of the physical specimen has the effect of reducing the restoring force. The restoring force measured and returned from the physical specimen to the hybrid model includes the effects from both mechanical and temperature commands. However, if the numerical element was also heat sensitive, the physical specimen thermal flux at the boundary with the numerical element would need to be measured and returned to the hybrid model. This would constitute two-way interaction between the numerical and experimental substructures. Two-way coupling at the microscopic scale would also be necessary (solving both the heat transfer to structural elements and mechanical response together). This is a topic for future TMHS implementations.

OpenSees and OpenFresco

OpenSees and OpenFresco, in their original versions, do not consider temperature DOFs, nor is a differential equation other than that of motion readily solvable given the current assembly and solution methods. Therefore, for implementing TMHS, the challenge was to create the notion of temperature DOFs within the existing OpenSees and OpenFresco frameworks without redefining the OpenSees domain and replicating all of the relevant classes in both frameworks.

Consider a two-dimensional truss element that experiences both thermal and mechanical loads. In the global coordinate system, a two-dimensional truss element has two mechanical DOFs at each node. A temperature DOF is associated with each face of the element at each node. Assuming a uniform temperature field at each end of the element, a two-dimensional element requires one temperature DOF per node. Fig. 1(a) shows the four mechanical DOFs and two temperature DOFs for the two-dimensional truss element in the global coordinate system. Fig. 1(b) shows the basic coordinate system, which has only one mechanical DOF (element elongation), and the two temperature DOFs.

The temperature DOFs must be accounted for in the dynamic equilibrium equations of the structural model in one of two ways: (1) as loads through the induced non-mechanical strains, or (2) as parameters that modify the mechanical properties of the structural model materials. In either implementation, the temperatures are not dependent on the outcome of the mechanical response analysis. In the current implementation of TMHS, the temperatures are

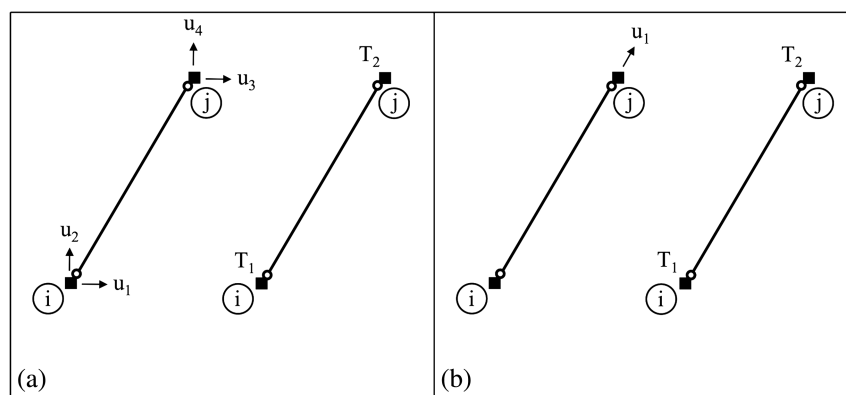


Fig. 1. Mechanical and thermal degrees of freedom: (a) global coordinate system; (b) basic coordinate system

treated as parameters that vary with time according to the prescribed temperature-time history, $T(t)$. The temperatures remain static during a time step but are updated between steps using an existing OpenSees parameter update procedure (Scott and Haukaas 2008). The temperature DOF values are carried in an expanded vector of displacement DOFs in OpenSees, but the temperature DOFs are not assembled into the global system of equilibrium equations.

This solution minimizes required changes in the existing OpenSees and OpenFresco frameworks and unnecessary divergence of the class hierarchy due to duplicated element and material classes, while remaining compatible with the recently developed temperature-dependent OpenSees material classes (Jiang and Usmani 2013). Additionally, this solution provides the means to accommodate a variable number of temperature DOFs. This capability is important to interface with temperature application systems (furnace controllers) that use more than one temperature feedback instrument, enabling application of a temperature differential across a specimen.

TMHS Architecture

OpenFresco is based on a client-server architecture. Fig. 2(a) shows a typical, local, mechanics-only implementation of OpenFresco. The Client includes the finite-element software, which is OpenSees in this case, and the following OpenFresco software classes (with abbreviations in parenthesis): experimental element (*ExpElement*), experimental site (*ExpSite*), experimental setup (*ExpSetup*), and experimental control (*ExpControl*). The Backend Server includes the control and data acquisition (DAQ) systems in the laboratory, which drive the physical specimen and acquire feedback quantities.

In Fig. 2(a), the OpenFresco *ExpElement*, which is a subclass of the *Element* class in OpenSees, provides the link between OpenSees and OpenFresco. The *ExpElement* then communicates with the experimental site. The main function of *ExpSite* is facilitating distributed hybrid simulation tests between multiple laboratory sites. In a local test, described herein, the experimental site simply transfers data between the experimental element and the experimental setup. *ExpSetup* transforms between the experimental

element DOFs in OpenFresco (usually in the basic system) and the actuator DOFs in the laboratory. *ExpControl* interfaces with the control and DAQ system in the laboratory to send actuator commands and to receive experimental feedback quantities.

Fig. 2(b) shows the OpenSees/OpenFresco architecture, modified to implement the TMHS method. This architecture is designed by first considering the requirements for testing the physical specimen in the laboratory. An Indel CPU board stand-alone master (SAM) is used as the digital signal processor (DSP), responsible for generating displacement and temperature command signals and receiving feedbacks from both the UTM and furnace. Because the Indel SAM was not supported in OpenFresco, a new Indel experimental control object, *ECIndel*, is developed. The *ECIndel* object design is based on the existing *ECdSpace* experimental control object, extended to control temperatures in addition to displacements.

In the TMHS architecture in Fig. 2(b), *ECIndel* is instantiated twice (through multiple realizations of the same concrete-derived class), once for displacement control and once for temperature control. An *ExpSetup* object is needed to interface with each *ExpControl* object. These are shown as the One Actuator setup (*ESOneActuator*) and the Thermal Simple setup (*ESThermalSimple*). The existing *ESOneActuator* experimental setup object is used to handle displacement DOFs. A new experimental setup object, *ESThermalSimple*, is developed to handle the temperature DOFs. The two experimental setups refer to the same element, so they are linked using the existing Aggregator setup (*ESAggregator*), which is modified to communicate temperatures with the new *ESThermalSimple* object and to rectify communication issues between the base class and the overloaded methods. The experimental site object, *LocalExpSite*, is unchanged. A new experimental element object, *EETrussThermal*, is implemented to support both mechanical and thermal loads.

Table 1 summarizes the sizes of the vectors that are passed from OpenSees through the OpenFresco classes during the hybrid simulation. OpenSees contains a vector with one mechanical DOF (the model only contains a single mechanical DOF) and two temperature DOFs (at the end nodes of the experimental element) in the global system. This vector gets passed as an input to

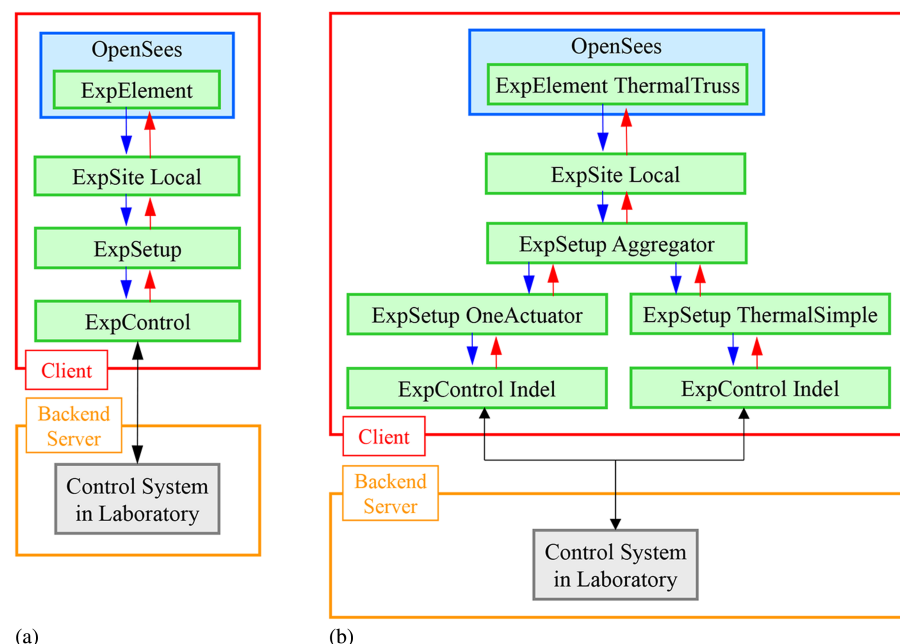


Fig. 2. (a) OpenFresco/OpenSees architecture; (b) TMHS OpenFresco/OpenSees architecture

Table 1. Mechanical and Temperature Input and Output Vector Sizes

OpenFresco class	Input/output vector sizes	
	Mechanical	Temperature
<i>EETrussThermal</i>	1/1	2/2
<i>LocalExpSite</i>	1/1	2/2
<i>ESOneActuator</i>	1/1	—
<i>ESThermalSimple</i>	—	2/3
<i>ECIndel disp</i>	1/1	—
<i>ECIndel temp</i>	—	3/3

Note: — = not applicable.

EETrussThermal, where it transforms the displacements to the basic system. This transformation does not affect the size of the vector in this case, so the output from *EETrussThermal* is also one mechanical DOF and two temperature DOFs. The size of the one mechanical DOF in the vector remains unchanged as it passes through all the OpenFresco classes. The only transformation occurs with temperature in *ESThermalSimple*. In the hybrid model in OpenSees, temperatures are specified at the two end nodes of the experimental element, but the laboratory furnace controls the temperature via a thermocouple mounted on the specimen at mid-height. Thus, *ESThermalSimple* calculates the average of the temperatures at the end nodes of the experimental element and provides three temperatures as output. The temperatures at the end nodes of the experimental element are not used for the proof-of-concept tests, but they are carried in the vector. After applying a displacement and a temperature to the physical specimen, the measured resisting force and temperature are sent back to OpenSees and transformed back to the global coordinate system of the structural model. However, the resisting force vector and stiffness matrix are assembled only for the mechanical DOF.

Laboratory Test Setup and Physical Specimen

Fig. 3 shows photographs of the laboratory test setup and physical specimen. Fig. 3(a) shows the Grade S355 structural steel dogbone-shaped physical specimen mounted in the combined Zwick 1484 UTM and Könn STE-12 HR/350° Electrical Furnace (Könn Furnace). This specimen is identical to a specimen tested in Series M8 RHS 120-60-3.6 by Pauli et al. (2012). The UTM grips the ends

of the specimen from above and below and can only apply tensile loads in this configuration. The dimensions of the narrow portion of the dogbone specimen, visible between the grips, are 75 mm long, 10 mm wide, and 3.6 mm thick. Three Type K thermocouples are shown with their connecting wires and are labeled in the figure with arrows. One thermocouple is located at specimen midheight and the other two are located in the upper and lower grips. The prescribed temperatures are applied to the specimen (not to the air temperature) and are controlled using the thermocouple at specimen midheight.

Two ceramic probes are shown contacting the specimen. In the view in Fig. 3(b), these probes are visible as part of the Maytec PMA-12/V7 extensometer, which is a device that controls the strain of the physical specimen directly. The ceramic material is important because it can withstand heating without undergoing deformation. UTM displacements do not provide accurate displacement feedback from the physical specimen in a fire test because the grips that hold the specimen are temperature sensitive, making it impossible to isolate the portion of the elongation that comes from the specimen. Therefore, use of the extensometer to measure the specimen deformations directly is essential.

Fig. 3(c) shows a global view of the testing configuration with the furnace doors closed. Here, the vertically mounted actuator can be seen. Load is applied to the specimen by moving the bottommost plate downward. The direction of loading is noted in the figure. The load cell, with a capacity of $+/- 200$ kN, is located below the furnace, in line with the actuator, and is also labeled. This test setup existed in the ETH Zürich laboratory prior to TMHS implementation. In the original configuration, displacements (or forces) and temperatures are prescribed in the Zwick/Roell testXpert II Software. Displacement (or force) commands are sent to the Zwick UTM. Temperature commands are sent to three West 8,100+ Single Loop Controllers, one for each temperature control zone, which in turn send commands to the Könn Furnace. The furnace has an 1,100°C maximum temperature, and is capable of heating at a rate of 60°C/min up to 600 and 40°C/min up to 1,100°C. While the TMHS framework is designed to enable real-time testing, the low heater power of the Könn Furnace was not able to achieve the target heating rates.

For the TMHS tests, the Zwick/Roell testXpert II Software is programmed to receive external control displacements and

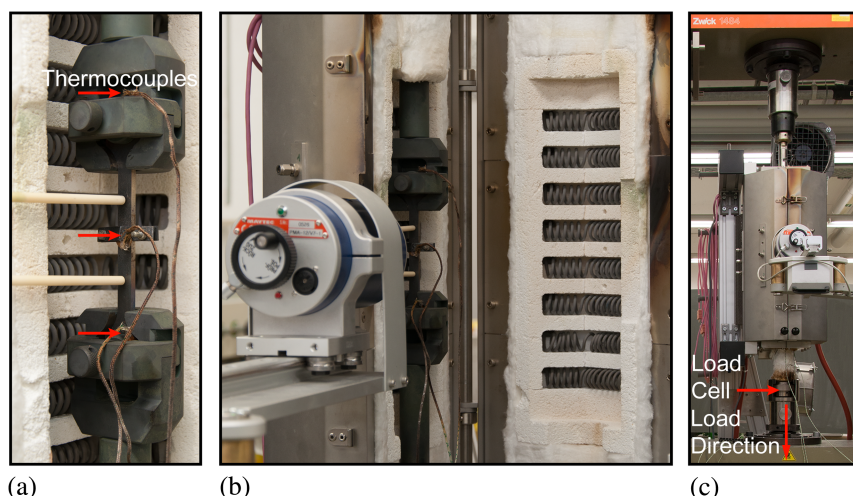


Fig. 3. (a) Steel dogbone-shaped physical specimen mounted in the Zwick UTM and Könn Furnace; (b) inside view of furnace with Maytec extensometer; (c) global view of the testing configuration with the furnace doors closed

temperatures through a digital communications (COM) port. The Indel SAM sends these at the required 1,000 Hz rate. After applying displacements and temperatures to the physical specimen, analog displacement, force, and temperature feedback measurements are returned to the Indel SAM. The testing velocity, PID gains, and force limits are provided internally in the Zwick/Roell testXpert II Software.

Three-Loop Control

The TMHS employs a three-loop hardware architecture strategy for hybrid simulation control, based on Mosqueda (2003) and Stojadinovic et al. (2006). Fig. 4 shows this TMHS architecture. The outermost loop is the integrator loop. Here, OpenSees and OpenFresco solve for target displacements and temperatures at an integration time step (dt_{int}) equal to simulation time divided by the prescribed number of substeps. For the proof-of-concept tests, $dt_{int} = 0.25$ s. The innermost loop is the servo-control and thermal-control loop. Here, the Zwick UTM and Könn Furnace control the displacements and temperatures of the physical specimen at a controller time step (dt_{con}) of 1/1,000 s (1,000 Hz). The middle loop contains the Indel SAM DSP and serves to bridge these two time steps. The Indel SAM runs a Simulink Model that receives the commands from OpenSees and OpenFresco and extrapolates them at the necessary 1/1,000 s time step. This can be accomplished using a variety of strategies such as a predictor-corrector algorithm. For the proof-of-concept tests, the displacements and temperatures are simply ramped to the next target values, and command signals are sent to the Zwick UTM and Könn Furnace at the appropriate rate. In the case of a delay in the system, the current displacement and temperature are held. After each displacement and temperature pair is achieved, the Indel SAM must receive the displacement, force, and temperature feedbacks and return them to OpenSees and OpenFresco.

The tasks of the Indel SAM are handled using a system of flags set by *ECIndel* and by the Simulink Model when certain states in the hybrid model are achieved. This strategy is replicated from the OpenFresco *ECdSpace* object and its corresponding Simulink Model. When a new target displacement is available, *ECIndel* sets a *newTarget* flag. The Simulink Model reads this flag and begins the ramp to that new target displacement. When the target displacement is reached, the Simulink Model sets an *atTarget* flag. *ECIndel* then commands the Simulink Model to read the restoring force.

The *newTargetThermal* and *atTargetThermal* flags work similarly for temperature commands. In each step, a displacement and a temperature are commanded, and both the *atTarget* and the *atTargetThermal* flags have to be achieved to move on to the next step. In this manner, the displacements and temperatures are applied at the appropriate times. In each step, *ECIndel* first waits for the *atTargetThermal* flag and then the *atTarget* flag. By alternating between confirming that temperature and displacement are achieved in each step, this ensures that both commands will remain appropriately synchronized. If there is a delay in the system, then neither the displacements nor temperatures will advance.

Hybrid Model and Proof-of-Concept TMHS Tests

Testing Protocol

The prototype structure for the proof-of-concept TMHS tests is a long-span girder fixed at both ends and supported at midspan by a hanger that is exposed to a fire. The hybrid model utilizes symmetry and comprises one-half of the girder (Element A) and the hanger (Element B) with a half of the prototype hanger area (Fig. 5). All loads and responses are presented referring to this two-element hybrid model. Nodes 1 and 3 are fully restrained, and the horizontal and rotational DOFs of Node 2 are restrained. Thus, the vertical displacement at Node 2 is the only free DOF. The beam element, A, is modeled numerically in OpenSees as a steel *elasticBeamColumn* and remains at room temperature throughout the test (no thermal loads are applied to it). Its stiffness in bending is $12EI/L^3$ because the rotation is fixed at Node 2. Its stiffness is chosen to be one-fourth of the measured axial initial stiffness of the physical column specimen. This value of one-fourth was selected after a few trials, so that the numerical element would not take the entire load when the physical specimen softened as it was heated. The experimental element, B, is represented in the hybrid model by the new OpenFresco *EETrussThermal* experimental element.

Fig. 5 shows the mechanical and thermal loading scheme for the TMHS tests. The duration of the proof-of-concept simulations is 30 s. There are 120 integration steps, so the simulation time step is $dt_{int} = 0.25$ s. The controller velocities are set at a strain rate of 0.2%/min (0.0015 mm/s) for displacement and 1°C/s for temperature in terms of wall-clock time. Because the furnace controller was often slow to respond to a new temperature command, this

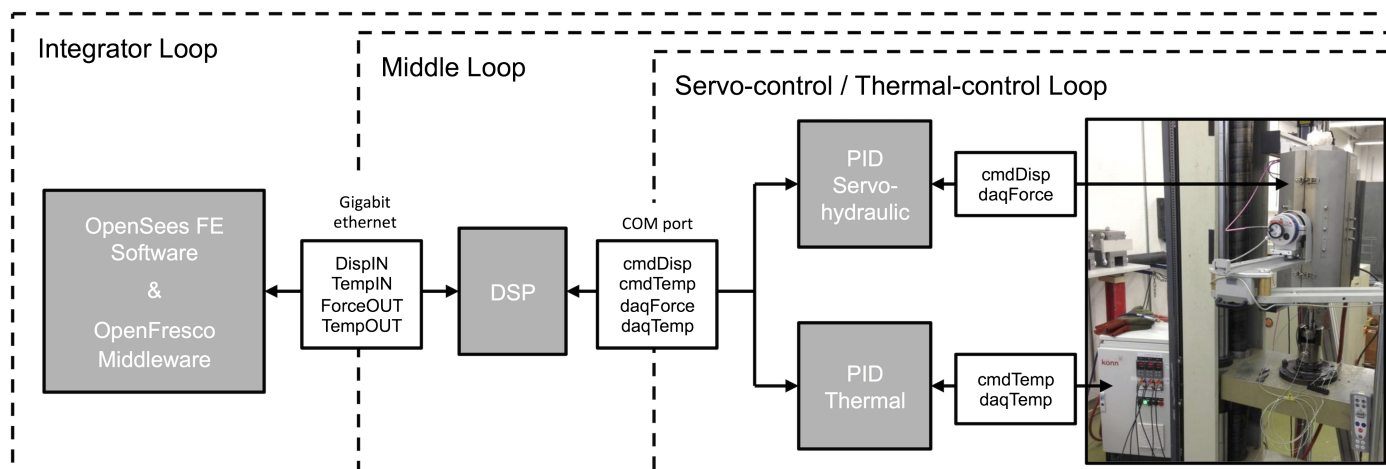


Fig. 4. TMHS three-loop hardware architecture

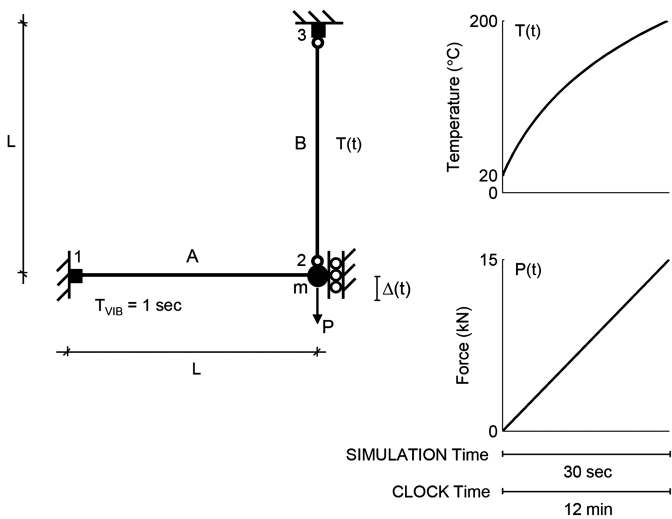


Fig. 5. Hybrid model with mechanical and thermal loading scheme

limited the speed of the test to 24 times slower than real time, lasting 12 wall-clock min. However, as mentioned previously, the TMHS method ensures that the displacements and temperatures proceed together, resulting in a slowdown in the event of a furnace delay. The load ramp and the temperature curve are designed so that the physical specimen does not experience any nonlinear behavior, and the test can be repeated many times using the same specimen. This strategy was used because many simulations were needed for developing and implementing TMHS. A force, $P(t)$, mechanically loads the hybrid model that ramps linearly from 0 to 15 kN over the course of the test. Simultaneously, element B is loaded thermally with a scaled version of the standard ISO 834 temperature-time fire load, $T(t)$. The scaling factor is adjusted with respect to the starting room temperature so that a final temperature of 200°C is achieved on the surface of the specimen at the end of each TMHS test. The analyses are performed with a dynamic integrator to enable future simulations of dynamic actions on structures in fire (e.g., earthquake followed by fire scenarios). To define the dynamic properties of the hybrid model, the fundamental vibration period of the hybrid model is selected to be 1 s, and the necessary mass is calculated and assigned in the numerical portion of the hybrid model. A 5% mass proportional Rayleigh damping is incorporated into the hybrid model.

Two integration schemes are used for the proof-of-concept tests: the Explicit Newmark Method (*NewmarkExplicit* where $\alpha = 0.5$, $\beta = 0$) and the Implicit Newmark Method with an increment reduction modification (*NewmarkHSIncrReduct* where $\gamma = 0.5$, $\beta = 0.25$, and reduction factor = 0.4) (Schellenberg 2008). For the implicit method, the number of iterations is fixed at 4 per time step. With implicit integrators, the physical specimen is affected by all substep iterations. If the integration method first applies a large displacement command and then a number of smaller displacement corrections, the physical specimen experiences undesirable, numerically induced accelerations. Another undesirable situation occurs if the first iteration overshoots, and then the next iterations pull the specimen back and cause numerically induced oscillations. Because these oscillations are not part of the actual specimen response, they should be minimized. The *NewmarkHSIncrReduct* reduction factor reduces the displacement command, such that the displacements are applied in a smooth, controller manner in each step, instead of as a large initial displacement substep, followed by very small displacement correction iterations.

Lessons Learned

Displacement controlled hybrid simulation of a structure's dynamic response in a thermal environment was a challenging problem for two reasons. The first difficulty was with designing the mechanical and the thermal loading schemes in a compatible way. As the specimen moved in displacement control in response to the mechanical loads, it elongated and its load increased. As the temperature in the furnace chamber increased, the specimen also elongated, but the displacement controlled hybrid simulation restrained this elongation, and the specimen's load decreased. Because the testing apparatus was designed for tensile loads only, the testing parameters had to be carefully balanced so the specimen did not experience compression during heating. Furthermore, because elastic response was desired, the physical specimen could not exceed its 14 kN yield force.

As mentioned previously, the integrator solves the equation of motion that describes the hybrid model, and the effect of increasing temperature on the physical specimen is captured in the measurement of the restoring force. The second implementation difficulty is that the integrator treats the restoring force as a constant value within each step (only changing between steps), but the furnace is continuously heating, so the force actually decreases throughout each step. The integrator computes a target displacement, but by the time the target displacement is applied to the physical specimen, the specimen has unloaded somewhat in response to the increasing temperature. Thus, the computed displacement is not consistent with the measured restoring force in that same step. In the first TMHS tests performed, this problem was very dramatic such that the analysis became unstable within the first few time steps without using a very large numerical damper to control the oscillations. The problem was caused by the initial *ECIndel* object implementation that checked the displacement flag first and the temperature flag second in each step. At the start of the next step predicted by the integrator, the restoring force corresponded to the force measured half a step previously (the measured force was too high); in the meantime, the temperature had increased and the force had dropped. This discrepancy caused an instability.

By changing the order of flag checking to temperature first and displacement second, the restoring force is measured at the end of a step and immediately used for the calculation in the next step, so the stability problem is resolved. However, there is still a discrepancy because the displacement is applied first, then the specimen force continues to drop from the thermal effect, and then the force is measured at the end of the step. The measured force is now too low. This causes the target displacements for the next step to overshoot. Thus, the solution of the response of the hybrid model oscillates, but remains stable.

This behavior is worsened by the slow speed of the hybrid simulation. In future tests, the thermal commands will be sent from the Indel directly to the furnace, bypassing the Zwick controller and furnace controller to increase the simulation speed in terms of clock time, and the force reduction within a step from the continued heating of the specimen will produce a less dramatic oscillatory effect. Furthermore, in future simulations with large-scale specimens and longer heating exposure, a furnace with a higher heating rate will be necessary to avoid any effects of specimen creep that might otherwise be induced by much slower than real-time heating rates.

The TMHS architecture supports more complex numerical and experimental substructures with more DOFs. The physical specimen in the proof-of-concept tests was a thin steel specimen, so surface and internal specimen temperature fields were assumed to be the same. With selection of a thicker cross section, this assumption would no longer be adequate, and internal specimen temperatures

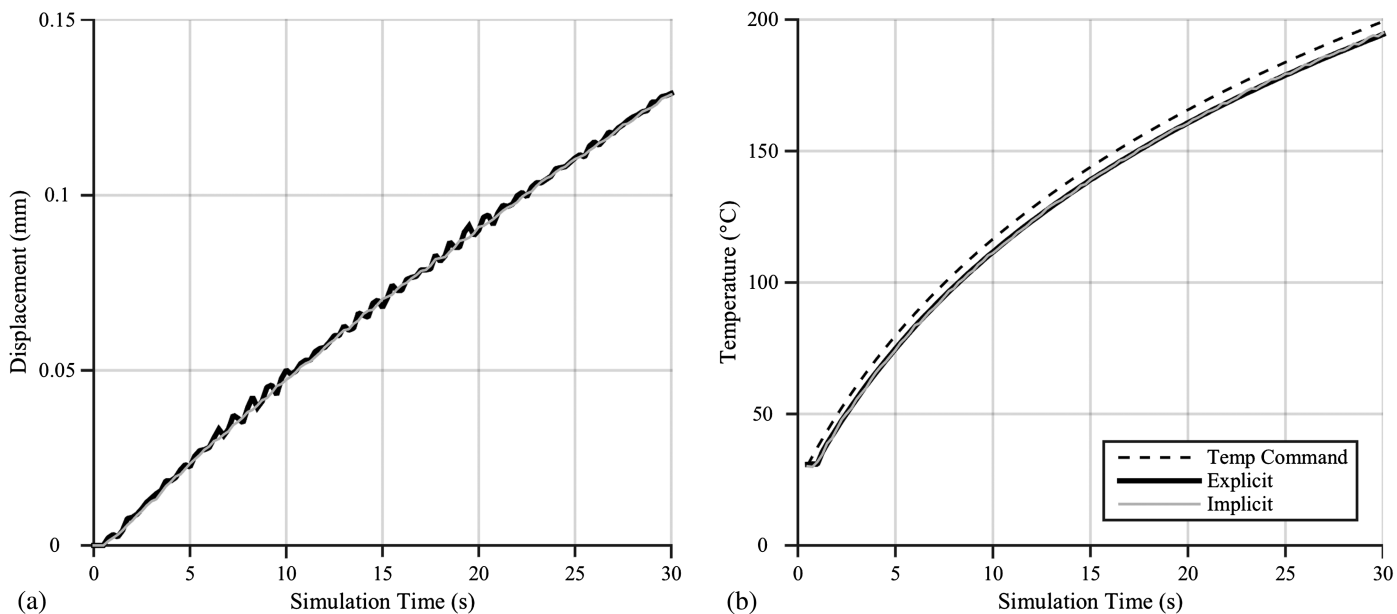


Fig. 6. (a) Displacement time history; (b) temperature time history (including command history) for the explicit and implicit integration methods

would have to be used for feedback. This is not a limitation of the TMHS method, but only a simplification for the proof-of-concept tests.

Results of the Proof-of-Concept TMHS Tests

The initial stiffness of the physical hanger specimen is experimentally measured and then updated in the hybrid model prior to each TMHS test. The stiffness test is performed by loading the specimen to 8 kN (smaller than its 14 kN yield force) and then unloading it at room temperature (approximately 20°C). The stiffness is calculated to be approximately 160 kN/mm using the slope

between the 2- and 6-kN data points, and it did not degrade between the tests.

Figs. 6(a and b) show the displacement and the temperature time history feedbacks for the explicit and the implicit integration methods, respectively. The explicit method introduces slightly more oscillations because it does not benefit from the reduction factor that was used for the implicit method. Figs. 7(a and b) show the force displacement history for the experimental element and for the numerical element for the explicit and the implicit integration methods, respectively. The TMHS results obtained using the two integration methods match well.

The quality of the servo-hydraulic displacement control is assessed by computing the differences between command and

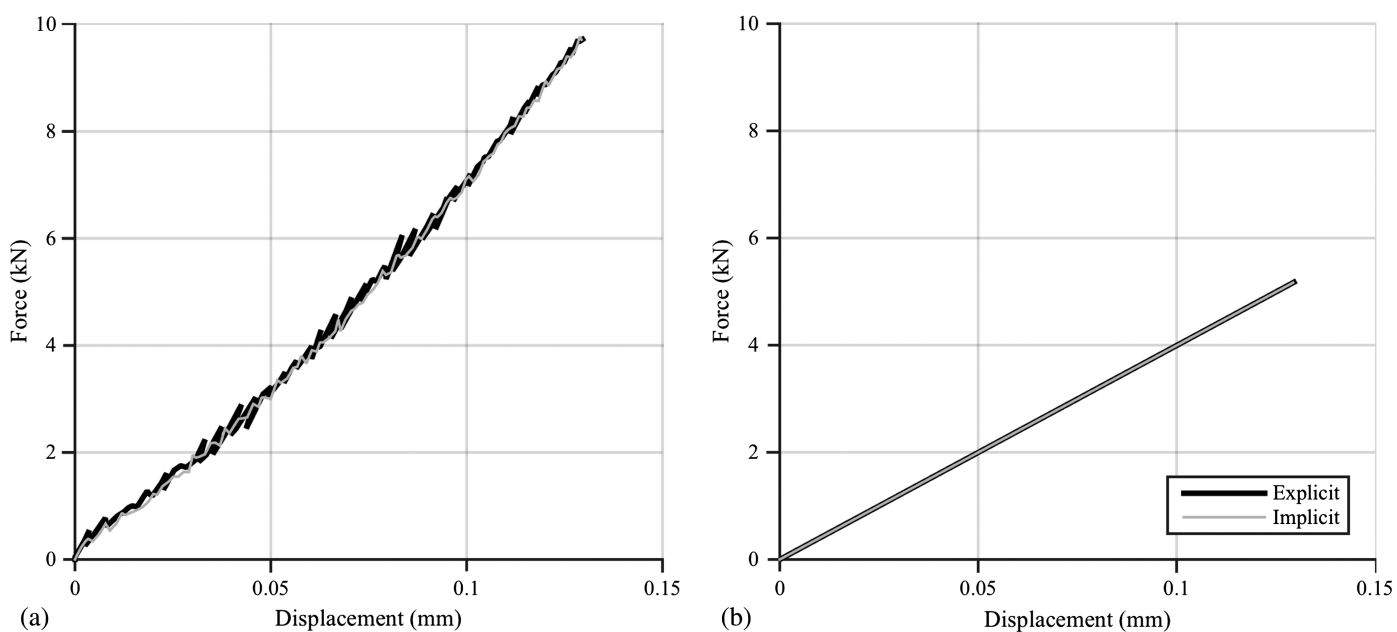


Fig. 7. Force displacement history for the explicit and implicit integration methods for: (a) experimental element; (b) numerical element

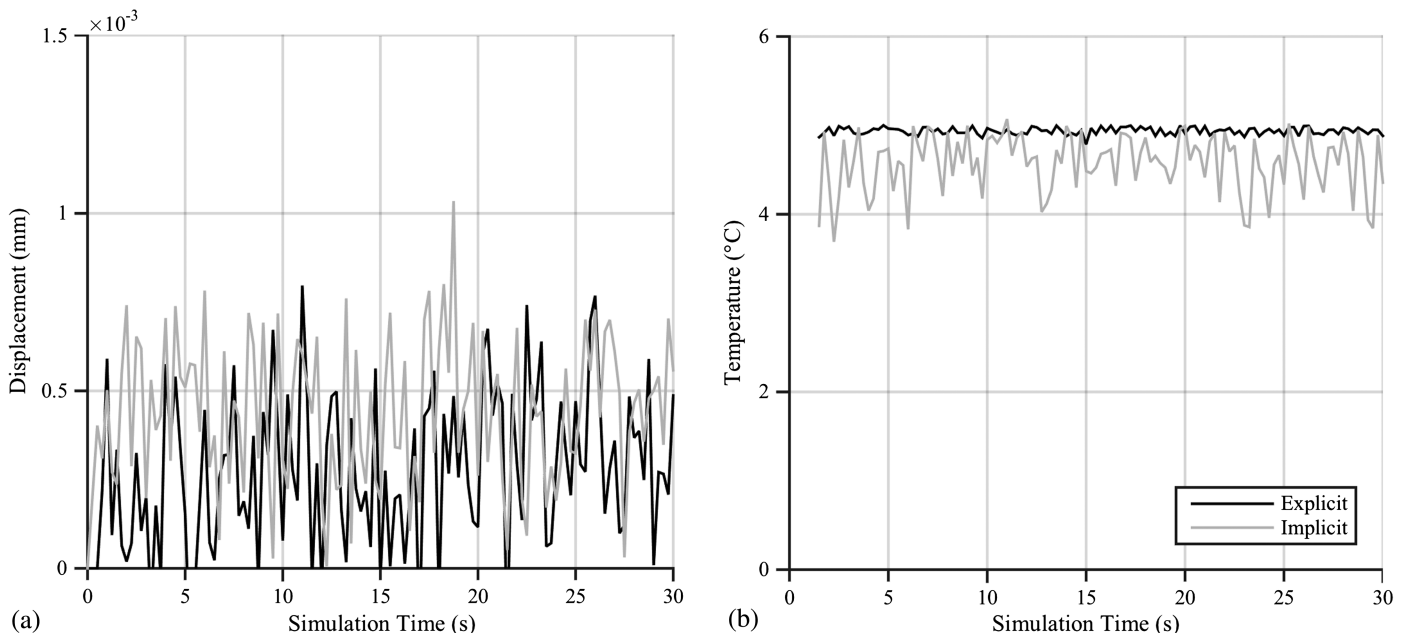


Fig. 8. (a) Displacement control errors; (b) thermal control errors for the explicit and implicit integration methods

feedback displacements. The errors are plotted in Fig. 8(a) for the explicit and the implicit TMHS tests. The displacement feedbacks are slightly lagging behind the displacement command signals, but the displacement errors remain small (approximately 0.001 mm compared to the maximum displacement of approximately 0.13 mm). The Simulink Model running on the Indel SAM checks that the feedback displacement is within the user specified tolerance of the command displacement at the end of each step. Satisfying this tolerance requirement is a prerequisite for moving onto the next step. The same check is performed for temperature commands as well. The error between temperature commands and feedbacks is shown in Fig. 8(b) for the

explicit and implicit test temperature controls. The feedback temperatures are lagging behind the command temperatures by about 5°C, which is a user-specified tolerance.

Fig. 9(a) shows the force displacement history for the full hybrid model's only DOF for the explicit integration method compared to the theoretical solution. Fig. 9(b) shows the same data for the implicit integration method. The theoretical solution is obtained by solving the statically indeterminate hybrid model using the same temperature load on the hanger at each time step that was measured in the TMHS. The thermal strain of the hanger is modeled as linearly proportional to the change in its temperature with the coefficient of thermal expansion $\alpha = 11.45 \times 10^{-6} \text{ m/m/}^{\circ}\text{C}$.

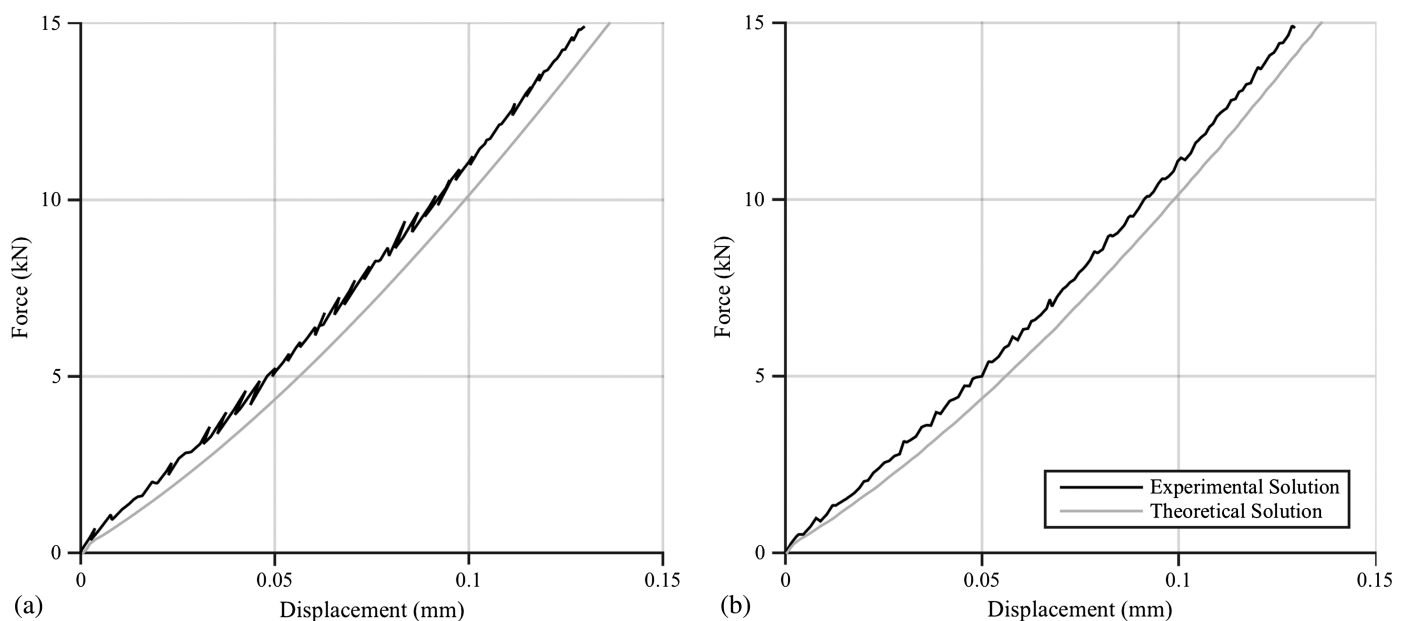


Fig. 9. Force displacement history compared to theoretical solution using the (a) explicit integration method; (b) implicit integration method

This is the average of the measured α values from the Series M8 tests by Pauli et al. (2012). The modulus of elasticity and the yield strength of the hanger material (steel) are kept at values corresponding to the room temperature because their reduction in the temperature range of this test (20°C up to 200°C) is smaller than 10% (Chen et al. 2006; Outinen 2007; Lee et al. 2013). The apparent hardening behavior in the solution is a result of the different rates of thermal elongation throughout the test. Because of the shape of the standard ISO 834 fire load curve [Eq. (1)], the temperatures, and thus the thermal elongation of the hanger element, increase more rapidly at the beginning of the test, and less so as the test proceeds.

The results of the TMHS proof-of-concept tests match the theoretical solution well for both integration methods. This validates the TMHS implementation. Furthermore, this close match shows the high quality (low error) of the TMHS test. The small discrepancy between the experimental and theoretical solutions is due to the parameters assumed in the numerical model, such as stiffness, area, and/or gauge length of the experimental member. Also, the measured physical specimen surface temperatures (assumed to be the same as the interior element temperatures) are used as the input interior element temperatures when calculating the theoretical solution. Therefore, the interior temperature of the physical specimen in the theoretical solution is modeled as too hot and produces more displacement than is observed in the experimental results. This highlights the importance of performing tests with experimental substructures: the theoretical solution does not capture the actual experimental behavior perfectly even with small loads and low temperatures. Because the hybrid model is a simple structure and the tests were slow so that the load and the temperature changed gradually, the explicit and the implicit integration schemes are expected to give the same results, as they did. For future tests with models that are more complex or experience nonlinear behavior, an implicit method will be necessary for numerical stability. An explicit method would require an unreasonably small time step.

Summary and Conclusions

A new TMHS method is presented, which is the result of a significant investment in the development of both the software and hardware needed to support combined mechanical and thermal loading on hybrid structures. TMHS provides a platform for cost-effective testing, which will enable expanded research on structures in fire beyond the typical component tests of single structural element responses to fire loads. The TMHS method extends the mechanical hybrid simulation method by incorporating temperature DOFs in the OpenFresco hybrid model domain and developing new OpenFresco objects and a test execution strategy to simultaneously control the elements of the experimental setup, the thermal loads, and the mechanical loads.

The implementation of the TMHS method at the ETH Zürich IBK Structural Testing Laboratory was verified and validated using a simple two-element hybrid model. The response of the model to simultaneously applied force ramp and a scaled version of the ISO 834 standard fire curve was obtained in two TMHS tests, one conducted using an explicit and the other using an implicit integration scheme. The test results are very similar, and both simulations match the theoretical solution well.

Challenges for future development of the TMHS method and opportunities for improved implementation abound. Further work is needed to minimize the observed oscillations in the displacement solution of the hybrid model by investigating the integrators' dependence on the thermomechanical problem and fine-tuning the simulation sequence to match the power of the available

mechanical and thermal test setups. New developments in furnace capabilities, such as more accurately applying and controlling varying temperature fields at higher heating rates and configurability to enclose specimens of varying geometry, are needed to match similar capabilities available for applying mechanical loads. Implementing a force control option, including switching control modes on the same DOF and mixed control across different DOFs (Elkhorabi and Mosalam 2007; Kim et al. 2010), should have a high priority to enable simulations that include materially and geometrically nonlinear response of the physical portion of the hybrid model.

Increasing the complexity of the numerical portion of the hybrid model requires improving the thermal modeling capabilities in OpenSees and accounting for two-way coupling, at least at the microscopic level. In future simulations, thermal flux equilibrium will be enforced at the experimental substructure interface, so the thermal flux feedbacks will be utilized in adjacent heat-transfer-enabled numerical substructure elements. Including a FDA and two-way coupling at the macroscopic level would be necessary to capture the interactions between mechanically induced damage and development of a fire.

Despite the challenges, the TMHS method proposed herein represents a significant step forward in the ability to conduct realistic simulations of the response of structures to extreme loads. The TMHS method offers a unique way to apply and control the thermal and mechanical boundary conditions of the fire-tested substructure in accordance with the numerically modeled thermal and mechanical time-history response of the remainder of the structure. Thus, the proposed method enables a significant increase in realism and complexity of structural fire resistance tests and opens the doors toward investigating the performance of structures in common multi-hazard situations such as fire after an earthquake or fire after an explosion.

Acknowledgments

The authors are grateful to Mr. Dominik Werne and Mr. Martin Neuenschwander of ETH Zürich for their valuable assistance with preparing the testing equipment. They appreciate OpenFresco code support from Dr. Andreas Schellenberg of University of California, Berkeley and discussions of test data with Prof. Nicola Tondini of University of Trento. ETH Zürich provided funding for this project. Any opinions, findings, and conclusions expressed herein are those of the authors and do not necessarily reflect the view of the ETH Zürich.

References

- CEN (European Committee for Standardization). (2002). "Eurocode 1: Actions on structures—Part 1-2: General actions—Actions on structures exposed to fire." *EN1991-1-2*, Brussels, Belgium.
- Chen, J., Young, B., and Uy, B. (2006). "Behavior of high strength structural steel at elevated temperatures." *J. Struct. Eng.*, **10.1061/(ASCE)0733-9445(2006)132:12(1948)**, 1948–1954.
- Chen, M., et al. (2012). "Design and construction of a full-scale 5-story base isolated building outfitted with nonstructural components for earthquake testing at the UCSD-NEES facility." *Proc., ASCE Structures Congress*, Chicago.
- Dwaikat, M. M. S., Kodur, V. K. R., Quiel, S. E., and Garlock, M. E. M. (2011). "Experimental behavior of steel beam-columns subjected to fire-induced thermal gradients." *J. Constr. Steel Res.*, **67**(1), 30–38.
- Elkhorabi, T., and Mosalam, K. M. (2007). "Towards error-free hybrid simulation using mixed variables." *Earthquake Eng. Struct. Dyn.*, **36**(11), 1497–1522.

- Franssen, J. M., et al. (1995). "A simple model for the fire resistance of axially-loaded members according to Eurocode 3." *J. Constr. Steel Res.*, 35(1), 49–69.
- Garner, L., and Baddoo, N. R. (2006). "Fire testing and design of stainless steel structures." *J. Constr. Steel Res.*, 62(6), 532–543.
- Jiang, J., and Usmani, A. (2013). "Modeling of steel frame structures in fire using OpenSees." *Comput. Struct.*, 118, 90–99.
- Kim, H., Whyte, C. A., and Stojadinovic, B. (2010). "Mixed and switch degree-of-freedom control in hybrid simulation." *Proc., 9th U.S. National and 10th Canadian Conf. on Earthquake Engineering*, Toronto.
- Kirby, B. R. (1997). "Large scale fire tests: The British Steel European collaborative research programme on the BRE 8-storey frame." *Proc., 5th Int. Symp.*, International Association for Fire Safety Science, Boston, 1129–1140.
- Kitano, T., et al. (2000). "Large scale fire tests of a 4-story type car park. Part 1: The behavior of structural frame exposed to the fire at the deepest part of the first floor." *Proc., 4th Asia-Oceania Symp. on Fire Science and Technology*, Tokyo.
- Lawson, J. R. (2009). "A history of fire testing." *Technical Note 1628*, Building and Fire Research Laboratory, National Institute of Standards and Technology, U.S. Dept. of Commerce, Gaithersburg, MD.
- Lee, J., Morovat, M. A., Hu, G., Engelhardt, M. D., and Taleff, E. M. (2013). "Experimental investigation of mechanical properties of ASTM A992 steel at elevated temperatures." *AISC Eng. J.*, 50(4), 249–272.
- Lie, T. T. (1989). "Fire resistance of reinforced concrete columns: A parametric study." *J. Fire Prot. Eng.*, 1(4), 121–129.
- Mahin, S. A., and Williams, M. E. (1981). "Computer controlled seismic performance testing." *2nd ASCE-EMD Specialty Conf. on Dynamic Response of Structures*, Atlanta.
- Martins, A. M. B., and Rodrigues, J. P. C. (2010). "Fire resistance of reinforced concrete columns with elastically restrained thermal elongation." *Eng. Struct.*, 32(10), 3330–3337.
- McClamroch, N. H., Serakos, J., and Hanson, R. D. (1981). "Design and analysis of the pseudo-dynamic test method." *Technical Rep. UMEE 81R3*, Univ. of Michigan, Ann Arbor, MI.
- Mosqueda, G. (2003). "Continuous hybrid simulation with geographically distributed substructures." Ph.D. dissertation, Univ. of California, Berkeley, CA.
- Mostafaei, H. (2013a). "Hybrid fire testing for assessing performance of structures in fire—Application." *Fire Saf. J.*, 56, 30–38.
- Mostafaei, H. (2013b). "Hybrid fire testing for assessing performance of structures in fire—Methodology." *Fire Saf. J.*, 58, 170–179.
- OpenFresco. (2015). "Open framework for experimental setup and control." (<http://openfresco.neesforge.nees.org>) (Mar. 24, 2015).
- OpenSees. (2015). "Open system for earthquake engineering simulation." (<http://opensees.berkeley.edu>) (Mar. 24, 2015).
- Outinen, J. (2007). "Mechanical properties of structural steels at elevated temperatures and after cooling down." *Proc., 10th Int. Meeting of Fire and Materials*, Interscience Communications, London.
- Pauli, J., et al. (2012). "Experiments on steel columns under fire conditions." *Institute of Structural Engineering Technical Rep. 340*, Swiss Federal Institute of Technology, Zurich, Switzerland.
- Saouma, V. E., and Sivaselvan, M. V. (2008). *Hybrid simulation: Theory, implementation and applications*, Taylor and Francis, London.
- Schellenberg, A. (2008). "Advanced implementation of hybrid simulation." Ph.D. dissertation, Univ. of California, Berkeley, CA.
- Scott, M. H., and Haukaas, T. (2008). "Software framework for parameter updating and finite-element response sensitivity analysis." *J. Comput. Civ. Eng.*, 10.1061/(ASCE)0887-3801(2008)22:5(281), 281–291.
- Stojadinovic, B., Mosqueda, G., and Mahin, S. A. (2006). "Event-driven control system for geographically distributed hybrid simulation." *J. Struct. Eng.*, 10.1061/(ASCE)0733-9445(2006)132:1(68), 68–77.
- Takanashi, K., Udagawa, K., Seki, M., Okada, T., and Tanaka, H. (1975). "Non-linear earthquake response analysis of structures by a computer-actuator on-line system." *Bulletin of Earthquake Resistant Structure Research Center*, Institute of Industrial Science, Univ. of Tokyo, Tokyo.
- Terzic, V., and Stojadinovic, B. (2014). "Hybrid simulation of bridge response to three-dimensional earthquake excitation followed by a truck load." *J. Struct. Eng.*, 10.1061/(ASCE)ST.1943-541X.0000913, A4014010-1–A4014010-14.
- Tondini, N., and Franssen, J.-M. (2013). "Implementation of a weak coupling approach between a CFD and an FE software for fires in compartment." *5th Int. Conf. on Computational Methods for Coupled Problems in Science and Engineering*, International Center for Numerical Methods in Engineering, Barcelona, Spain.
- Tondini, N., Rossi, B., and Franssen, J.-M. (2013). "Experimental investigation on ferritic stainless steel columns in fire." *Fire Saf. J.*, 62, 238–248.
- Wang, Y. C. (2002). *Steel and composite structures: Behaviour and design for fire safety*, Spon Press, New York.
- Whyte, C. A., and Stojadinovic, B. (2014). "Effect of ground motion sequence on the response of squat reinforced concrete shear walls." *J. Struct. Eng.*, 10.1061/(ASCE)ST.1943-541X.0000912, A4014004-1–A4014004-7.